New physics implications of vector boson fusion searches exemplified through the Georgi-Machacek model

Manimala Chakraborti,[1,*] Dipankar Das,[2,†] Nivedita Ghosh,[3,‡] Samadrita Mukherjee,[4,§] and Ipsita Saha[5,‖]

[1]*School of Physics and Astronomy, University of Southampton, Southampton, SO17 1BJ, United Kingdom*
[2]*Department of Physics, Indian Institute of Technology (Indore), Khandwa Road, Simrol, 453 552 Indore, India*
[3]*Centre for High Energy Physics, Indian Institute of Science, Bengaluru 560012, India*
[4]*Department of Theoretical Physics, Tata Institute of Fundamental Research, Mumbai 400005, India*
[5]*Department of Physics, Indian Institute of Technology Madras, Chennai 600036, India*

(Received 16 August 2023; accepted 15 December 2023; published 16 January 2024)

LHC searches for nonstandard scalars in vector boson fusion (VBF) production processes can be particularly efficient in probing scalars belonging to triplet or higher multiplet representations of the Standard Model $SU(2)_L$ gauge group. They can be especially relevant for models where the additional scalars do not have any tree level couplings to the Standard Model fermions, rendering VBF as their primary production mode at the LHC. In this work we employ the latest LHC data from VBF resonance searches to constrain the properties of nonstandard scalars, taking the Georgi-Machacek model as a prototypical example. We take into account the theoretical constraints on the potential from unitarity and boundedness from below as well as indirect constraints coming from the signal strength measurements of the 125 GeV Higgs boson at the LHC. To facilitate the phenomenological analysis we advocate a convenient reparametrization of the trilinear couplings in the scalar potential. We derive simple correlations among the model parameters corresponding to the decoupling limit of the model. We explicitly demonstrate how a combination of theoretical and phenomenological constraints can push the Georgi-Machacek model towards the decoupling limit. Our analysis suggests that the VBF searches can provide key insights into the composition of the electroweak vacuum expectation value.

DOI: 10.1103/PhysRevD.109.015016

I. INTRODUCTION

The remarkable success of the Standard Model (SM), culminating in the discovery of the 125 GeV Higgs scalar at the LHC, has fuelled further investigations into the understanding of the precise nature of electroweak symmetry breaking (EWSB). In the $SU(2)_L \times U(1)_Y$ gauge theory of the SM, the EWSB is driven by an $SU(2)_L$ scalar doublet in such a way that the electric charge Q, with $Q = T_{3L} + \frac{Y}{2}$, remains conserved [1,2]. A question that naturally arises in this context is whether there exist additional scalar multiplets of $SU(2)_L$ beyond the SM (BSM) that contribute to the mechanism of EWSB. If such a scenario is indeed realized in nature, the nonstandard scalars originating from an extended scalar sector are expected to possess trilinear couplings with a pair of massive SM gauge bosons (of the form $SV_1^\mu V_{2\mu}$) with strengths proportional to the vacuum expectation values (VEVs) of the extra multiplets. Thus, a straightforward way to look for such nonstandard scalars at the LHC is via their production in vector boson fusion (VBF) production processes, provided the BSM scenario in question can accommodate sizable trilinear couplings of the scalars to a pair of weak gauge bosons. In other words, the LHC searches for nonstandard scalar resonances in VBF production processes can potentially serve as a powerful tool to pin down any BSM contribution to the process of EWSB.

Nonstandard contribution to the electroweak VEV can arise only from the presence of scalar multiplets transforming nontrivially under the $SU(2)_L$ part of the SM, since $SU(2)_L$ singlet scalars, even if charged under the hypercharge gauge group $U(1)_Y$, do not participate in EWSB. In the popular multi-Higgs doublet extensions of

*mani.chakraborti@gmail.com
†d.das@iiti.ac.in
‡niveditag@iisc.ac.in
§samadrita.mukherjee@tifr.res.in
‖ipsita@iitm.ac.in

the SM Higgs sector, the tree level trilinear couplings of the nonstandard Higgs bosons to a pair of weak gauge bosons vanish in the well-known "alignment limit" of the model [3,4]. In this limit of multi-Higgs doublet models, the Higgs doublet fields can be rotated to the so-called Higgs basis where the electroweak VEV can be effectively allocated entirely to only one of the Higgs doublets, while the VEVs of all other doublets remain zero [5,6]. The chosen Higgs doublet with nonzero VEV can then give rise to the SM-like Higgs boson observed at the LHC [7,8]. Thus, the nonstandard scalars in the alignment limit do not possess any trilinear coupling to the weak gauge boson pairs. With the current experimental data pointing strongly towards the validity of the alignment limit [9], the possibility of a significantly large trilinear coupling of the nonstandard scalars to a pair of weak vector bosons seems to be thin on the ground. One must note here that the introduction of additional scalar singlets and doublets to the SM field content preserves the custodial $SU(2)$ symmetry and is therefore safe from the stringent constraints stemming from the precise measurement of electroweak ρ parameter.

Moving beyond the doublets, the next step will be to introduce an additional triplet scalar field into the SM scalar sector, giving rise to the so-called Higgs triplet model (HTM). Unlike the BSM scenarios with extra singlets and doublets, those involving triplets or higher multiplets of $SU(2)_L$, in general, have the tendency to modify the tree level value of the electroweak ρ parameter. For the HTM, the triplet VEV can significantly alter the tree level value of electroweak ρ parameter, making the model vulnerable to the constraints coming from precision electroweak measurements. The experimental determination of the electroweak ρ parameter, $\rho \approx 1$, severely restricts the VEV of the neutral component of the triplet to values less than a few GeV [10–12]. This tones down any potential enhancement in the trilinear couplings of the form $SV_1^\mu V_{2\mu}$ which are directly proportional to the triplet VEVs [13], thereby reducing their observability in the high energy collider experiments. Thus, in order to accommodate a substantially large triplet VEV in a BSM scenario the vacuum state of the model must be designed in such a way that it preserves the custodial symmetry. A prototypical theoretical framework within this class of constructions is provided by the Georgi-Machacek (GM) model [14–16]. In the GM model, the SM scalar sector is extended by introducing two additional triplet scalar fields (one complex and one real) which acquire equal VEVs. This leads to an internal cancellation of the custodial symmetry breaking effects, securing $\rho = 1$ at tree level. As a consequence of the unbroken custodial symmetry, the common triplet VEVs can now be sizable, allowing for significantly large trilinear couplings of the nonstandard Higgs bosons to the massive gauge boson pairs. Thus, the GM model can serve as the ideal candidate to illustrate the potential of VBF searches at the LHC in determining the basic ingredients of the electroweak VEV.

Several LHC searches have been designed specifically to look for VBF production of nonstandard scalars in diboson final states [17–21]. In this work, we use the latest results from the full LHC run-II dataset to constrain the properties of additional triplet scalars, within the example framework of GM model. The GM model consists of several nonstandard scalar bosons which can give rise to very distinctive phenomenologies at the colliders. The physical scalar spectrum of the model can be categorized into a number of custodial multiplets, namely, one fiveplet $(H_5^{++}, H_5^{+}, H_5^{0}, H_5^{-}, H_5^{--})$, one triplet $(H_3^{+}, H_3^{0}, H_3^{-})$, and two singlets h and H. One important feature of this model is that the members of the custodial fiveplet do not couple to the SM fermions at tree level. Thus, the dominant direct bounds on the common mass of the custodial fiveplet can be obtained from the LHC searches looking for nonstandard bosons in VBF production processes, making these searches tailor-made for this model. In addition to collider data, we also consider the theoretical constraints from perturbative unitarity and boundedness-from-below (BFB) conditions on the potential. A suitable reparametrization of the trilinear couplings of the scalar potential is prescribed, making way for efficient phenomenological analysis. We show that the decoupling limit of the GM model can be expressed in terms of simple correlations among the physical masses, mixing angles and the triplet VEV. We also take into consideration the bounds coming from the measurement of the properties of 125 GeV Higgs boson, which we identify as the lightest CP-even custodial singlet boson h present in the GM model. In our analysis, we demonstrate that the VBF searches can provide complementary constraints to the theoretical bounds on the model parameter space. We also give estimates for the potential of the future colliders such as the high luminosity (HL-)LHC, Future Circular colliders etc. to constrain the remaining parameter space further. We explicitly show that the projected limits from the HL-LHC VBF searches for new scalar resonances in combination with the theoretical constraints will practically push the GM model towards the decoupling limit, imposing stringent constraints on the triplet contribution to the electroweak VEV.

Analyses trying to constrain the GM model parameter space from the LHC run-II data have been performed earlier in the literature [22–37]. Our analysis supersedes them by including the full run-II dataset for the diboson resonance searches, some of which were not available during the time of the previous analyses. Apart from the direct collider searches, we employ the latest measurement of the trilinear Higgs self-coupling to provide complementary constraints on the GM model parameter space. Another important feature of our analysis is the simple parametrization of the input variables in terms of physical quantities

resulting in a more direct interpretation of the phenomenological results.

The plan of our paper is as follows. In Sec. II, we briefly review the GM model. In Sec. III, we discuss the theoretical constraints on the model from perturbative unitarity and BFB requirements of the potential. Here we also formulate correlations among the physical parameters corresponding to the decoupling limit of the model. Constraints from the 125 GeV Higgs signal strength measurements are described in Sec. IV A. In Sec. IV B we describe the impact of the direct search constraints from the LHC on the parameter space of the GM model. The prospect for future colliders like the HL-LHC to further constrain this scenario is discussed in Sec. IV C. Finally, we summarize our findings in Sec. V.

II. A BRIEF RECAP OF THE GM MODEL

The GM model extends the scalar sector of the SM, consisting of the $Y = 1$ complex doublet $\phi \equiv (\phi^+ \ \phi^0)^\intercal$, by adding two $SU(2)_L$ triplet scalar fields, one real $\xi \equiv (\xi^+ \ \xi^0 \ \xi^-)^\intercal$ and one complex $\chi \equiv (\chi^{++} \ \chi^+ \ \chi^0)^\intercal$, with hypercharges $Y = 0$ and $Y = 2$, respectively [14–16]. The scalar sector of this model is conventionally expressed in terms of a bidoublet Φ and a bitriplet X, defined as

$$\Phi = \begin{pmatrix} \phi^{0*} & \phi^+ \\ -\phi^- & \phi^0 \end{pmatrix}, \quad X = \begin{pmatrix} \chi^{0*} & \xi^+ & \chi^{++} \\ -\chi^- & \xi^0 & \chi^+ \\ \chi^{--} & -\xi^- & \chi^0 \end{pmatrix}. \tag{1}$$

The scalar potential for this model can be written as [27,38]

$$\begin{aligned} V(\Phi, X) = {} & \frac{\mu_\phi^2}{2}\mathrm{Tr}(\Phi^\dagger\Phi) + \frac{\mu_X^2}{2}\mathrm{Tr}(X^\dagger X) + \lambda_1[\mathrm{Tr}(\Phi^\dagger\Phi)]^2 + \lambda_2\mathrm{Tr}(\Phi^\dagger\Phi)\mathrm{Tr}(X^\dagger X) \\ & + \lambda_3\mathrm{Tr}(X^\dagger X X^\dagger X) + \lambda_4[\mathrm{Tr}(X^\dagger X)]^2 - \lambda_5\mathrm{Tr}(\Phi^\dagger\tau_a\Phi\tau_b)\mathrm{Tr}(X^\dagger t_a X t_b) \\ & - M_1\mathrm{Tr}(\Phi^\dagger\tau_a\Phi\tau_b)(UXU^\dagger)_{ab} - M_2\mathrm{Tr}(X^\dagger t_a X t_b)(UXU^\dagger)_{ab}, \end{aligned} \tag{2}$$

with $\tau_a \equiv \sigma_a/2$, $(a = 1, 2, 3)$, where σ_as are the Pauli matrices and t_as are the generators of the triplet representation of $SU(2)_L$ and are given by

$$t_1 = \frac{1}{\sqrt{2}}\begin{pmatrix} 0 & 1 & 0 \\ 1 & 0 & 1 \\ 0 & 1 & 0 \end{pmatrix}, \qquad t_2 = \frac{1}{\sqrt{2}}\begin{pmatrix} 0 & -i & 0 \\ i & 0 & -i \\ 0 & i & 0 \end{pmatrix}, \qquad t_3 = \begin{pmatrix} 1 & 0 & 0 \\ 0 & 0 & 0 \\ 0 & 0 & -1 \end{pmatrix}. \tag{3}$$

The matrix U appearing in the trilinear terms of Eq. (2) is given by

$$U = \frac{1}{\sqrt{2}}\begin{pmatrix} -1 & 0 & 1 \\ -i & 0 & -i \\ 0 & \sqrt{2} & 0 \end{pmatrix}. \tag{4}$$

After the EWSB, the neutral components of the bidoublet and the bitriplet are expanded around their VEVs as

$$\phi^0 = \frac{1}{\sqrt{2}}(v_d + h_d + i\eta_d), \qquad \xi^0 = (v_t + h_\xi),$$
$$\chi^0 = \left(v_t + \frac{h_\chi + i\eta_\chi}{\sqrt{2}}\right). \tag{5}$$

The requirement of equal VEVs to the real and the complex triplets ensures that custodial symmetry in the scalar potential remains intact. From the expressions of W and Z boson masses, the electroweak VEV can be identified as

$$\sqrt{v_d^2 + 8v_t^2} = v = 246 \text{ GeV}. \tag{6}$$

Thus, there will be two independent minimization conditions for the scalar potential corresponding to the two VEVs of the bidoublet and the bitriplet (v_d and v_t). These can be used to extract the bilinear coefficients of the potential μ_ϕ^2 and μ_X^2 in terms of v_d and v_t as follows:

$$\mu_\phi^2 = -4\lambda_1 v_d^2 - 3(2\lambda_2 - \lambda_5)v_t^2 + \frac{3}{2}M_1 v_t, \tag{7a}$$

$$\mu_X^2 = -(2\lambda_2 - \lambda_5)v_d^2 - 4(\lambda_3 + 3\lambda_4)v_t^2 + \frac{M_1 v_d^2}{4v_t} + 6M_2 v_t. \tag{7b}$$

Now, the bilinear terms in the scalar potential can be diagonalized to obtain the physical Higgs scalars of the model which can be classified according to their transformation properties under the custodial SU(2) as a quintuplet $(H_5^{++}, H_5^+, H_5^0, H_5^-, H_5^{--})$ with common mass m_5, a triplet (H_3^+, H_3^0, H_3^-) of common mass m_3 and two custodial singlets, h and H with masses m_h and m_H, respectively. In this article, we refrain ourselves from giving a detailed description of the diagonalization

procedure and we refer the reader to Refs. [38,39]. The mass eigenstates for the charged and neutral scalars are defined below[1]:

$$H_5^{\pm\pm} = \chi^{\pm\pm}, \tag{8a}$$

$$H_5^{\pm} = \frac{1}{\sqrt{2}}(\chi^{\pm} - \xi^{\pm}), \tag{8b}$$

$$H_5^0 = \sqrt{\frac{2}{3}}h_\xi - \sqrt{\frac{1}{3}}h_\chi,$$

$$H_3^{\pm} = -\sin\beta\ \phi^{\pm} + \frac{\cos\beta}{\sqrt{2}}(\chi^{\pm} + \xi^{\pm}), \tag{8c}$$

$$H_3^0 = -\sin\beta\,\eta_d + \cos\beta\,\eta_\chi, \tag{8d}$$

$$h = \cos\alpha\,h_d + \sin\alpha\,H_5^{0\prime}, \tag{8e}$$

$$H = -\sin\alpha\,h_d + \cos\alpha\,H_5^{0\prime}, \tag{8f}$$

where

$$H_5^{0\prime} = \sqrt{\frac{1}{3}}h_\xi + \sqrt{\frac{2}{3}}h_\chi. \tag{9}$$

The angle α represents the mixing angle in the neutral Higgs sector while $\tan\beta$ is defined as

$$\tan\beta = \frac{2\sqrt{2}v_t}{v_d}. \tag{10}$$

It can be observed from Eq. (8) that the members of the custodial fiveplet are composed entirely of $SU(2)_L$ scalar triplets without any admixture from the doublets. Considering the fact that the SM fermions can couple only to the doublet component, the members of the custodial fiveplet will not have any tree-level coupling to the SM fermions. Thus, the dominant production mode available for these particles at the LHC is via the VBF process, making the VBF searches essential to probe the properties of such particles.

Before closing this section we note from Eq. (2) that there are nine parameters in the GM scalar potential with two bilinears (μ_ϕ^2 and μ_χ^2), five quartic couplings (λ_i, $i = 1, \ldots, 5$), and two trilinear couplings (M_1 and M_2). Among these, the bilinears can be replaced by the VEVs, v_d and v_t using Eq. (7). The five quartic couplings can also be exchanged for the four physical scalar masses, m_5, m_3, m_H, and m_h and the mixing angle, α. Below, we present the relation between the λ_is with the physical masses and mixings [27]:

$$\lambda_1 = \frac{1}{8v^2\cos^2\beta}\left(m_h^2\cos^2\alpha + m_H^2\sin^2\alpha\right), \tag{11a}$$

$$\lambda_2 = \frac{1}{12v^2\cos\beta\sin\beta}\left(\sqrt{6}(m_h^2 - m_H^2)\sin 2\alpha + 12m_3^2\sin\beta\cos\beta - 3\sqrt{2}v\cos\beta M_1\right), \tag{11b}$$

$$\lambda_3 = \frac{1}{v^2\sin^2\beta}\left(m_5^2 - 3m_3^2\cos^2\beta + \sqrt{2}v\cos\beta\cot\beta M_1 - 3\sqrt{2}v\sin\beta M_2\right), \tag{11c}$$

$$\lambda_4 = \frac{1}{6v^2\sin^2\beta}\left(2m_H^2\cos^2\alpha + 2m_h^2\sin^2\alpha - 2m_5^2 + 6\cos^2\beta m_3^2 - 3\sqrt{2}v\cos\beta\cot\beta M_1 + 9\sqrt{2}v\sin\beta M_2\right), \tag{11d}$$

$$\lambda_5 = \frac{2m_3^2}{v^2} - \frac{\sqrt{2}M_1}{v\sin\beta}. \tag{11e}$$

We wish to reiterate that in our analysis we consider h to be the lightest CP-even scalar corresponding to the Higgs boson discovered at the LHC with mass $m_h \approx 125$ GeV. In this study we will focus on the VBF production of the nonstandard GM scalars at the LHC.

[1]Note that our convention of α differs from that of Ref. [38] by a negative sign.

III. THEORETICAL CONSTRAINTS AND THE DECOUPLING LIMIT

To motivate the benchmark choices for our phenomenological analysis later, it is important to discuss the implications of the theoretical constraints from tree unitarity and BFB [38,40]. We will present our observations in terms of the physical masses and mixings and focus on formulating a systematic method to approach the SM-like limit also known as the decoupling limit [38]. It is quite intuitive that the decoupling limit will be achieved when $v_t \ll v$ and all the nonstandard scalars are much heavier than the

electroweak scale. Since this has been already discussed in Ref. [38], we will be brief and report only the important relations relevant to our present study. The distinct upshot of our analysis is that the relations we obtain involve only the physical parameters and therefore are quite straightforward to implement into the numerical codes, giving us a greater control over the parameters required for the phenomenological studies.

To begin with, we suggestively reparametrize the trilinear coupling parameters M_1 and M_2 as follows:

$$\Lambda_1^2 = \frac{M_1 v}{\sqrt{2}\sin\beta} \equiv \frac{M_1 v^2}{4 v_t}, \tag{12a}$$

$$\Lambda_2^2 = 3\sqrt{2} v M_2 \sin\beta \equiv 12 v_t M_2. \tag{12b}$$

With these reparametrizations let us now investigate the unitarity conditions. Theoretical constraints from perturbative unitarity put upper bounds on the eigenvalues of the $2 \to 2$ scalar scattering amplitude matrix. The eigenvalues can be expressed in terms of certain independent combinations of the scalar quartic couplings, given as [38,40]

$$x_1^{\pm} = 12\lambda_1 + 14\lambda_3 + 22\lambda_4 \pm \sqrt{(12\lambda_1 - 14\lambda_3 - 22\lambda_4)^2 + 144\lambda_2^2}, \tag{13a}$$

$$x_2^{\pm} = 4\lambda_1 - 2\lambda_3 + 4\lambda_4 \pm \sqrt{(4\lambda_1 + 2\lambda_3 - 4\lambda_4)^2 + 4\lambda_5^2}, \tag{13b}$$

$$y_1 = 16\lambda_3 + 8\lambda_4, \tag{13c}$$

$$y_2 = 4\lambda_3 + 8\lambda_4, \tag{13d}$$

$$y_3 = 4\lambda_2 - \lambda_5, \tag{13e}$$

$$y_4 = 4\lambda_2 + 2\lambda_5, \tag{13f}$$

$$y_5 = 4\lambda_2 - 4\lambda_5. \tag{13g}$$

The theoretical constraints from perturbative unitarity requires that each of these eigenvalues must obey the condition $|x_i^{\pm}|, |y_i| \leq 8\pi$.

To illustrate the implications of the decoupling limit, we take the example of $|y_2| \leq 8\pi$ that, in terms of the physical parameters, reduces to

$$\left| \frac{1}{3}[m_5^2 + 2(m_h^2 \sin^2\alpha + m_H^2 \cos^2\alpha)] - m_3^2 \cos^2\beta \right| \leq 2\pi v^2 \sin^2\beta. \tag{14}$$

In the decoupling limit when $v_t \ll v$, i.e., $\sin^2\beta \ll 1$, the above relation will be extremely constraining and will effectively reduce to the following equality:

$$\frac{1}{3}[m_5^2 + 2(m_h^2 \sin^2\alpha + m_H^2 \cos^2\alpha)] - m_3^2 \cos^2\beta \approx 0. \tag{15}$$

The conditions $|y_1| \leq 8\pi$ and $|y_3 - y_5| \leq 16\pi$ will also have similar implications which we do not show explicitly.[2]

Another type of constraint will arise from conditions like $|y_3| \leq 8\pi$, which reduces to

$$\left| m_3^2 - \frac{\sqrt{2}}{\sqrt{3}}(m_H^2 - m_h^2)\frac{\sin 2\alpha}{\sin 2\beta} \right| \leq 4\pi v^2. \tag{16}$$

Similar constraints can be obtained from $|y_4|, |y_5| \leq 8\pi$. A common feature of all these constraints is the occurrence of the ratio $(\sin 2\alpha / \sin 2\beta)$ which blows up in the limit $\sin\beta \ll 1$ and thus jeopardizes the unitarity conditions for $m_H^2 \gg v^2$. Therefore, imposition of the unitarity conditions will entail a correlation between $\sin\alpha$ and $\sin\beta$ so that constraints like Eq. (16) can be satisfied even for $v_t \ll v$. From the example conditions of Eqs. (15) and (16), one may intuitively infer that the unitarity conditions will be trivially satisfied for

$$\sin 2\alpha \approx \sqrt{\frac{3}{2}} \sin 2\beta \quad \text{with} \quad v_t \ll v \tag{17a}$$

$$\text{and} \quad m_H^2 \approx m_3^2 \approx m_5^2 \approx \Lambda_1^2 \gg v^2; \qquad \Lambda_2^2 \ll v^2, \tag{17b}$$

Equation (17) defines the decoupling limit in the GM model. Using the definition of $\tan\beta$ in Eq. (10), we may simplify Eq. (17) as

$$\sin\alpha \approx 2\sqrt{3}\frac{v_t}{v}, \tag{18}$$

which will often be used as benchmark for our phenomenological analysis. A visual confirmation of Eq. (17) is given in Fig. 1 where we see that, for $v_t \ll v$, heavy nonstandard scalars beyond the TeV scale would require $\sin\alpha$ to be strongly correlated to v_t. Such a correlation is not unique to the GM model and can be found in the usual HTM as well [41].

It should be noted that, in the decoupling limit defined by Eq. (17), the quartic couplings of Eq. (11) take much simpler forms as follows:

$$\lambda_1 \approx \frac{m_h^2}{8v^2}, \qquad \lambda_2 \approx \lambda_5 \approx 0. \tag{19}$$

Thus, only some of the quartic coefficients survive in the decoupling limit and λ_1 approaches the SM value. Additionally, since the doublet-triplet mixing is also vanishingly small in the decoupling limit, the physical scalar h, defined in Eq. (8e), will have SM-like couplings and can play the role of the SM-like Higgs boson observed at the

[2]The conditions $|y_3|, |y_5| \leq 8\pi$ can be combined to obtain $|y_3 - y_5| \leq 16\pi$ using the triangle inequality.

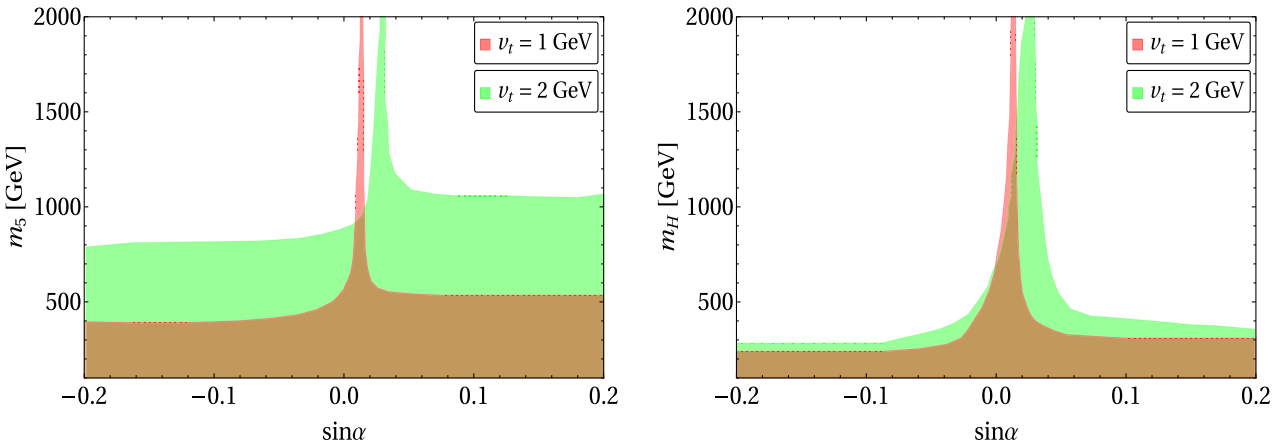

FIG. 1. Allowed regions from the combined constraints of unitarity and BFB in the limit $v_t \ll v$. The location of the narrow peak correspond to the decoupling limit defined by Eq. (17).

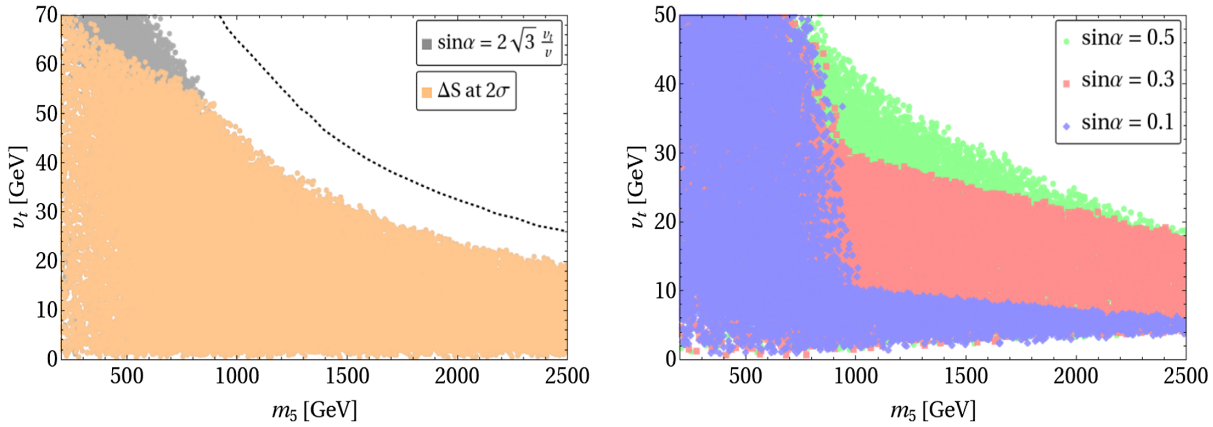

FIG. 2. Points allowed by the theoretical constraints of perturbative unitarity and BFB constraints. In the left panel we have assumed Eq. (18) to correlate $\sin\alpha$ and v_t. The dashed black line represents the conservative bound given by Eq. (23). In the right panel different benchmark values of $\sin\alpha$ are chosen, which are unrelated to v_t. The different colors in the right panel correspond to different values of $\sin\alpha$ mentioned in the legends. The gray points in the left panel are excluded when we impose the additional constraint from ΔS. As can be seen from the left panel, the constraint from ΔS starts to become relevant for $v_t \gtrsim 50$ GeV. In the right panel, ΔS does not impose any additional restriction for the displayed region of parameter space.

LHC [7,8]. Also comparing Eqs. (12a) and (17b) we see that a small triplet VEV is intimately connected to large nonstandard scalar masses, which carries the reminiscence of a type II seesaw mechanism.

Another interesting point to note from Eqs. (12) and (17) is that the trilinear coupling M_1 plays a crucial role in ensuring safe decoupling of the nonstandard scalars. Therefore, variants of the GM model without the trilinear couplings M_1 and M_2, do not have a decoupling limit and therefore can be ruled out rather easily [27].

Next we display in Fig. 2 the points that pass the combined constraints arising from unitarity and BFB. We exhibit results for the cases when Eq. (18) is satisfied as well as when $\sin\alpha$ and v_t are unrelated. If $\sin\alpha$ and v_t are unrelated then, as expected, the decoupling limit cannot be achieved and as a result we see in the right panel of Fig. 2 that a substantial area in the low v_t region is excluded. We would like to comment here that our result agrees with Ref. [38] with regards to the exclusion from the perturbative unitarity and BFB requirements. The forbidden region in the upper right corners of Fig. 2 can be qualitatively understood from the trilinear couplings of the Higgs bosons with a pair of W bosons. Let us express these couplings as follows[3]:

$$\mathcal{L}^{\text{tri}}_{WWS} = gM_W W^+_\mu W^{\mu-}(\kappa^h_W h + \kappa^H_W H + \kappa^{H_5}_W H^0_5) + gM_W \frac{\kappa_2}{2}(W^+_\mu W^{\mu+} H^{--}_5 + \text{H.c.}), \tag{20}$$

[3]Note that H^0_3 being a pseudoscalar does not possess coupling of the form $H^0_3 W^+_\mu W^{\mu-}$.

where S represents a generic scalar, g denotes the $SU(2)_L$ gauge coupling strength and the κs are given as

$$\kappa_W^h = \left(\sqrt{\frac{8}{3}}\sin\alpha\sin\beta + \cos\alpha\cos\beta\right), \tag{21a}$$

$$\kappa_W^H = \left(\sqrt{\frac{8}{3}}\cos\alpha\sin\beta - \sin\alpha\cos\beta\right), \tag{21b}$$

$$\kappa_W^{H_5} = \frac{\sin\beta}{\sqrt{3}}, \tag{21c}$$

$$\kappa_2 = \sqrt{2}\sin\beta. \tag{21d}$$

It is instructive to verify that these coupling modifiers obey the unitarity sum rule [42]

$$(\kappa_W^h)^2 + (\kappa_W^H)^2 + (\kappa_W^{H_5})^2 = 1 + (\kappa_2)^2. \tag{22}$$

The Lee-Quigg-Thacker bound on the Higgs boson masses [43], in this context, should thus read

$$(\kappa_W^h)^2 m_h^2 + (\kappa_W^H)^2 m_H^2 + \left[(\kappa_W^{H_5})^2 + \frac{1}{2}(\kappa_2)^2\right] m_5^2 \leq 4\pi v^2. \tag{23}$$

This inequality gives rise to a conservative bound from perturbative unitarity which can qualitatively explain the forbidden region in the upper-right corner of Fig. 2. We show this bound as a black dashed line in the left panel of Fig. 2.

To make the notion of decoupling more explicit, we calculate the trilinear couplings of the SM-like Higgs, h, with a pair of charged scalars in the limit of Eq. (17). In particular, the factors that control the contributions of the charged scalar loops in decays like $h \to \gamma\gamma$ and $h \to Z\gamma$ are given by [44]

$$\kappa_{3+} \equiv \frac{v}{2m_3^2} g_{hH_3^+H_3^-} \approx -\frac{1}{m_3^2}(m_3^2 - \Lambda_1^2 + m_h^2), \tag{24a}$$

$$\kappa_{5+} \equiv \frac{v}{2m_5^2} g_{hH_5^+H_5^-} \approx -\frac{1}{m_5^2}(2m_5^2 - 3m_3^2 + \Lambda_1^2 - \Lambda_2^2 + m_h^2), \tag{24b}$$

$$\kappa_{5++} \equiv \frac{v}{2m_5^2} g_{hH_5^{++}H_5^{--}} \approx -\frac{1}{m_5^2}(2m_5^2 - 3m_3^2 + \Lambda_1^2 - \Lambda_2^2 + m_h^2), \tag{24c}$$

where Eq. (17a) has been assumed. Clearly, when Eq. (17b) is also imposed, we will have $\kappa_{3+}, \kappa_{5+}, \kappa_{5++} \approx 0$ implying that the charged scalars are decoupled from the loop-induced Higgs decays in the limit of Eq. (17), as expected. In this context it should be emphasized that the expressions of Eq. (24) crucially depend on how the limit $\sin\alpha \to 0$ is approached. For example, instead of Eq. (17a), if we first apply $\sin\alpha \approx 0$ independent of v_t and then take $v_t \ll v$, then we would obtain

$$\kappa_{3+} \approx -1, \tag{25a}$$

$$\kappa_{5+} \approx -\frac{1}{m_5^2}(3m_3^2 - 2\Lambda_1^2), \tag{25b}$$

$$\kappa_{5++} \approx -\frac{1}{m_5^2}(3m_3^2 - 2\Lambda_1^2), \tag{25c}$$

which do not lead to proper decoupling of the heavy charged scalars. Therefore, to ensure safe decoupling of the nonstandard scalars one must approach $\sin\alpha \to 0$ limit in the way dictated by Eq. (17a).

Here we wish to clarify the distinction between the notions of "alignment" and "decoupling." "Alignment" refers to the limit when the lighter neutral Higgs boson (h) originates entirely from the $SU(2)_L$ doublet (i.e., $\sin\alpha = 0$) making fermionic couplings of h to be SM-like.[4] Additionally, in this limit $v_t \ll v_d$ so that the $SU(2)_L$ triplet Higgses have negligible couplings of the form $SV_1^\mu V_{2\mu}$, making the trilinear $hV_1^\mu V_{2\mu}$ couplings to be SM-like as well. However, one of the crucial observations of our paper is that merely making the tree level couplings of h to be SM-like does not guarantee the decoupling of heavy scalars, as has been emphasized through our Eqs. (23) and (24). For proper decoupling, we should approach $\sin\alpha \to 0$ and $\sin\beta \to 0$ in a correlated manner. Such discussions of alignment vs decoupling are quite widespread for doublet extensions [44,45]. In this work we have performed a similar analysis for the triplet extensions, which has remained somewhat less explored in the literature so far.

We also wish to add that the discussion made in this section highlights an underemphasized fact that, in the scenario of superheavy nonstandard scalars (much heavier than the EW scale) with only the SM-like scalar at the EW scale, the perturbative unitarity constraints automatically push us towards the decoupling limit (in a spirit similar to Ref. [46]). Such an aspect of perturbative unitarity has been discussed earlier for multi-Higgs-doublet models [6,44,47] and the HTM [41]. Here we explicitly demonstrate the connection between perturbative unitarity and the

[4]Putting $\sin\alpha = 0$ in Eqs. (11b) and (11e), we obtain $4(2\lambda_2 - \lambda_5)v_t = M_1$. Note that, such a relation can also be inferred by demanding the off-diagonal element of the 2×2 mass matrix in the $h_d - H_5^{0\prime}$ basis [38] to be zero. However, if $\sin\alpha = 0$ limit is approached in this way, it will lead to alignment without decoupling.

decoupling limit for the GM model as well. We believe that this section will help to view the perturbative unitarity constraints in a new light and serve as a motivation for the parametrization that we advocate.

For later use, we also give the expression of the coupling modifier for the trilinear Higgs self-coupling, which reads

$$\kappa_\lambda \equiv \frac{\lambda_{hhh}}{(\lambda_{hhh})^{\rm SM}} = \cos^3\alpha\sec\beta + \frac{2\sqrt{2}}{\sqrt{3}}\sin^3\alpha\csc\beta + \frac{2\Lambda_1^2}{m_h^2}\sin^2\alpha\cos\beta\left(\cos\alpha - \frac{\sqrt{2}}{\sqrt{3}}\sin\alpha\cot\beta\right) + \frac{\sqrt{2}}{3\sqrt{3}}\frac{\Lambda_2^2}{m_h^2}\sin^3\alpha\csc\beta. \tag{26}$$

One can easily check that $\kappa_\lambda = 1$ in the limit of Eq. (17). Moving away from the decoupling limit, however, the deviation in λ_{hhh} can be significantly large depending on the parameter combinations. Preliminary measurements of κ_λ can already put important constraints on the model parameter space, as will be discussed in more detail in Sec. IV B.

In passing, we recall that the oblique S parameter [48] has been known to put important constraints on the parameter space of the GM model [24,49,50]. The new physics contribution to the S parameter in the GM model is given by [50],[5]

$$\begin{aligned}\Delta S &\equiv S^{\rm GM} - S^{\rm SM},\\ &\approx \frac{s_W^2 c_W^2}{\pi e^2}\left\{-\frac{e^2}{12 s_W^2 c_W^2}(\ln m_3^2 + 5\ln m_5^2) + 2|g_{ZhH_3^0}|^2 f_1(m_h, m_3)\right.\\ &\quad + 2|g_{ZHH_3^0}|^2 f_1(m_H, m_3) + 2(|g_{ZH_5^0H_3^0}|^2 + 2|g_{ZH_5^+H_3^-}|^2) f_1(m_5, m_3)\\ &\quad + |g_{ZZh}|^2\left[\frac{f_1(M_Z, m_h)}{2M_Z^2} - f_3(M_Z, m_h)\right] - |g_{ZZh}^{\rm SM}|^2\left[\frac{f_1(M_Z, m_h^{\rm SM})}{2M_Z^2} - f_3(M_Z, m_h^{\rm SM})\right]\\ &\quad + |g_{ZZH}|^2\left[\frac{f_1(M_Z, m_H)}{2M_Z^2} - f_3(M_Z, m_H)\right] + |g_{ZZH_5^0}|^2\left[\frac{f_1(M_Z, m_5)}{2M_Z^2} - f_3(M_Z, m_5)\right]\\ &\quad \left. + 2|g_{ZW^+H_5^-}|^2\left[\frac{f_1(M_W, m_5)}{2M_W^2} - f_3(M_W, m_5)\right]\right\},\end{aligned} \tag{27}$$

where e stands for the electric charge, $s_W(c_W)$ is the sine (cosine) of the weak mixing angle, M_Z is the Z-boson mass and g_{XYZ} denotes the coupling among the X, Y, and Z particles excluding the Lorentz factor. For explicit expressions of these couplings, we refer the reader to Refs. [38,50] where a sign difference in the definition of $\sin\alpha$ needs to be taken into account. The quantity $m_h^{\rm SM}$ is the reference value of the SM Higgs boson mass for which the fit value of the S parameter is obtained. The f_1 and f_3 functions are given as

$$f_1(m_X, m_Y) = \begin{cases} \dfrac{1}{36(m_X^2 - m_Y^2)^3}[5(m_Y^6 - m_X^6) + 27(m_X^4 m_Y^2 - m_X^2 m_Y^4) \\ \quad + 12(m_X^6 - 3m_X^4 m_Y^2)\ln m_X + 12(3m_X^2 m_Y^4 - m_Y^6)\ln m_Y], & \text{for } m_X \neq m_Y \\ \frac{1}{6}\ln m_X^2, & \text{for } m_X = m_Y \end{cases} \tag{28}$$

and

$$f_3(m_X, m_Y) = \begin{cases} \dfrac{m_X^4 - m_Y^4 + 2m_X^2 m_Y^2(\ln m_Y^2 - \ln m_X^2)}{2(m_X^2 - m_Y^2)^3}, & \text{for } m_X \neq m_Y \\ \dfrac{1}{6m_X^2}, & \text{for } m_X = m_Y \end{cases}. \tag{29}$$

At first glance the expression in Eq. (27) might seem strange because of the appearance of dimensionful quantities inside logarithms. However, the expression is meaningful because ΔS remains unaffected if all the mass-dimensionful quantities are multiplied by a common scale factor. This happens as a result of the following relation satisfied by the couplings

[5]It should be noted that this expression of ΔS relies on the assumption that the new physics scale is much larger than M_Z. Although it is possible to define the oblique parameters without this assumption [51,52], the corresponding expressions for the GM model do not seem to be available in the literature. Keeping this in mind, the results that follow from Eq. (27) should be interpreted with caution.

$$-\frac{e^2}{s_W^2 c_W^2}+\frac{2}{3}\{|g_{ZhH_3^0}|^2+|g_{ZHH_3^0}|^2+|g_{ZH_5^0H_3^0}|^2+2|g_{ZH_5^+H_3^-}|^2\}+\frac{1}{3M_W^2}|g_{ZW^+H_5^-}|^2$$
$$+\frac{1}{6M_Z^2}\{|g_{ZZh}|^2+|g_{ZZH}|^2+|g_{ZZH_5^0}|^2-|g_{ZZh}^{\mathrm{SM}}|^2\}=0. \quad (30)$$

For our numerical analysis, the fit value of ΔS has been taken to be [53]

$$\Delta S=-0.01\pm 0.07. \quad (31)$$

The impact of the ΔS constraints can be seen in the left panel of Fig. 2 where we show the points excluded at 2σ in gray. It can be seen that the ΔS constraints start becoming important for $v_t \gtrsim 50$ GeV. This observation holds even when the benchmarks of $\sin\alpha$ are chosen independently of v_t. Therefore, we do not explicitly show the excluded region in the right panel of Fig. 2. As we will see in Secs. IV A and IV B, such large values of v_t are already excluded by the collider constraints from the LHC.

IV. EXPERIMENTAL CONSTRAINTS

In this section we will describe the relevant experimental constraints on the parameter space of the GM model. First, we will discuss the constraints coming from the measurement of the 125 GeV Higgs signal strengths. After outlining the parameter space satisfying the theoretical constraints as described in Sec. III and the Higgs signal strength constraints, we will derive the most relevant direct search bounds from the LHC on the remaining parameter region. The future prospects for the HL-LHC will also be discussed.[6]

A. Constraint from Higgs signal strengths

The physical Higgs state h with mass $m_h \approx 125$ GeV in our scenario arises from the mixing between two custodial singlets. This mixing will cause the couplings of h with the massive fermions and gauge bosons to deviate from their corresponding SM values. Such deviations are tightly constrained by the precision measurements of the Higgs boson couplings at the LHC. Both the ATLAS [9] and CMS [54] collaborations have studied various production and decay modes of the 125 GeV Higgs boson, thereby giving limits on the signal strength observables defined as

$$\mu_j^i=\frac{\sigma^i}{(\sigma^i)_{\mathrm{SM}}}\times\frac{\mathrm{BR}_j}{(\mathrm{BR}_j)_{\mathrm{SM}}}, \quad (32)$$

where σ^i represents the production cross section in the ith mode and BR_j denotes the branching ratio into the final state j.

We depict our results in Fig. 3 which shows the range of allowed values for v_t with respect to $\sin\alpha$, as obtained after applying Higgs signal strength constraints. We show the regions allowed by the signal strengths for gluon-gluon fusion and VBF production modes as red and blue shaded regions, respectively. We consider constraints from the $f\bar{f}$ and VV final states, f and V being the generic symbols for massive SM fermions and vector bosons, respectively. Additionally, we also take into account the constraint from the $\gamma\gamma$ final state. The allowed parameter space thus corresponds to the common region covered by the red and blue shaded zones. The bottom line is that the Higgs signal strength data restricts v_t to a finite region, putting clearly defined upper and lower limits on it for a fixed $\sin\alpha$.

B. Direct search constraints from the LHC

As mentioned in the introduction, the presence of a rich variety of nonstandard scalars makes the GM model subject to various constraints coming from the nonstandard Higgs boson searches at the LHC. In this study we focus mostly on the potential impact of the bounds coming from the VBF production of the custodial fiveplet charged and neutral scalars. We also discuss direct search bounds on the custodial triplet and singlet nonstandard Higgs bosons, namely $H_3^\pm$, H_3^0, and H. In the following, we briefly

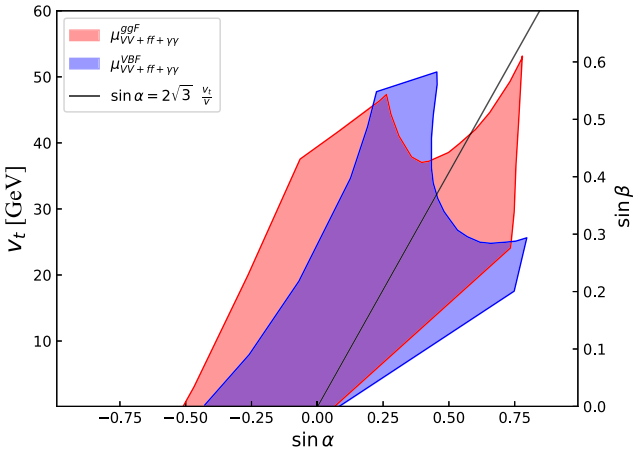

FIG. 3. Allowed parameter space from Higgs signal strength measurements at 95% confidence level (CL) [9,54]. For a fixed $\sin\alpha$, v_t is restricted to a finite region, with clear upper and lower limits.

[6]The indirect constraints from flavor data (especially from $b\to s\gamma$) start becoming relevant for $v_t \gtrsim 40$ GeV for all m_3 and m_5 [50]. As we shall see, this region of parameter space is excluded by the direct LHC searches for nonstandard scalars.

describe the most important direct searches considered by us in this analysis.

(1) The ATLAS collaboration has performed searches for the VBF production of a neutral heavy resonance S_0 decaying to Z-boson pairs in the leptonic final states [18]. The result is interpreted as a model-independent upper bound on the production cross section times branching ratio $(\sigma_{\rm VBF} \times {\rm BR}(S_0 \to ZZ))$ for the VBF production process as a function of the resonance mass. This data can be effective in constraining the neutral member of the custodial fiveplet H_5^0 as well as the custodial singlet H in the GM model.

(2) Searches for a charged Higgs boson have been performed in VBF production mode and its subsequent decay into $W^{\pm}Z$ modes [20] and the null results have been translated into exclusion bounds on the signal cross section as a function of the charged Higgs boson mass. This bound can be crucial to constrain the properties of the charged Higgs state $H_5^{\pm}$.

(3) The CMS collaboration has looked for the VBF production of a doubly charged scalar in like-sign WW final states, producing model independent bounds on the corresponding signal strength as a function of doubly charged Higgs mass [55]. Additionally, the Drell-Yan production of a pair of doubly charged Higgs bosons with decays to WW pairs has been investigated by the ATLAS collaboration [19]. We employ these data to constrain the properties of the $H_5^{\pm\pm}$ particle.

Apart from the direct LHC searches, we also discuss here the constraints coming from 125 GeV Higgs boson trilinear self-coupling measurements at the LHC [54,56–58]. Additionally, we checked our parameter space against the constraints on the quartic gauge-Higgs coupling modifier κ_{2V} [59] from di-Higgs production process [58]. This provides a much weaker bound compared to other constraints, excluding only $\sin\alpha \gtrsim 0.81$. Therefore, we do not explicitly show this constraint in the figures that follow.

We simulate the production of the nonstandard Higgs bosons via the VBF process and their subsequent decays using MadGraph-v-3.4.0 [60]. For this, we implement our model in FeynRules [61,62] which generates UFO files to be used by MadGraph5_aMC@NLO. The direct search limits are interpreted separately for the two mass hierarchies $m_5 < m_3$ and $m_5 > m_3$.

In Fig. 4 we show the combined effect of applying the bounds from theoretical constraints, Higgs signal strength data and the direct search limits from the LHC in the $m_5 - v_t$ plane for the mass hierarchy $m_5 < m_3$. The gray shaded region corresponds to parameter space excluded from theoretical constraints of unitarity and BFB, and the Higgs signal strength data. The collider bounds are then determined for the surviving parameter points. The blue and purple shaded regions are excluded from direct search constraints on H_5^0 in the ZZ decay mode [18] and $H_5^{\pm}$ in the $W^{\pm}Z$ final states [20], respectively. The exclusion limit from the VBF production of $H_5^{\pm\pm}$ decaying to two like-sign W bosons [55] is shown as a red shaded region. In Fig. 4, we depict our results for two benchmark values of $\sin\alpha$. Larger values of $\sin\alpha$, independent of the value of v_t, correspond to farther departure from the decoupling limit. Therefore, such $\sin\alpha$ values are expected to receive more stringent constraints from the LHC searches in general. As can be observed from the right panel of Fig. 4, the allowed parameter space is squeezed to a narrow region around the

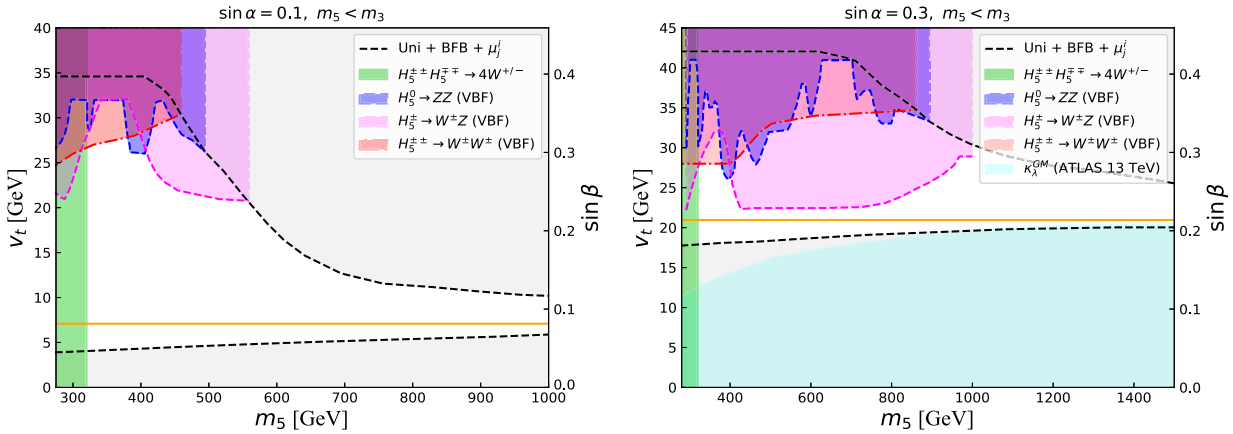

FIG. 4. Combined theoretical and experimental constraints on the $m_5 - v_t$ parameter plane for $m_5 < m_3$ hierarchy with $\sin\alpha = 0.1$ (left) and $\sin\alpha = 0.3$ (right). The excluded regions are shaded with various colors explained in the text. The orange solid line corresponds to the correlation $\sin\alpha = 2\sqrt{3}v_t/v$. Beyond the green band, the VBF searches dominate over Drell-Yan search channel and put nontrivial constraints on the parameter space.

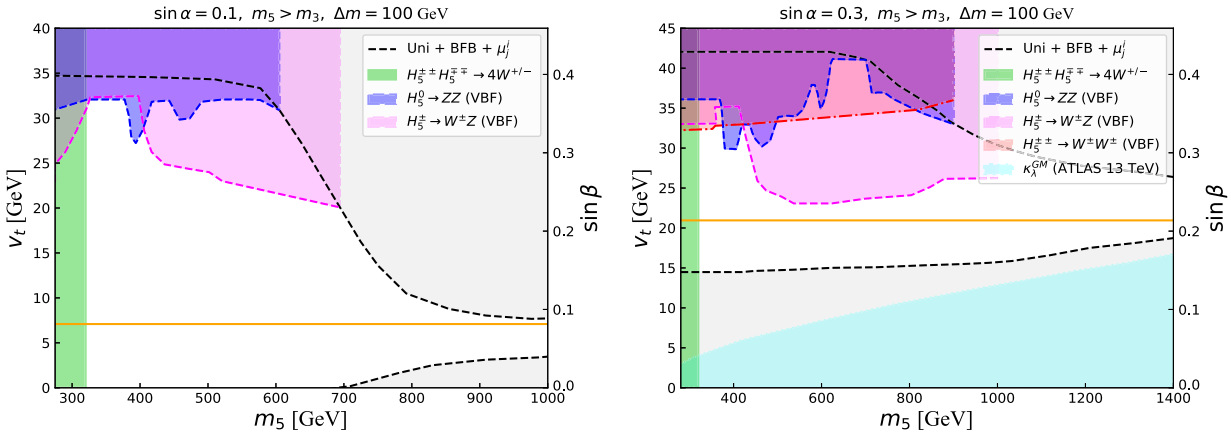

FIG. 5. Combined theoretical and experimental constraints on $m_5 - v_t$ parameter plane for $m_5 > m_3$ hierarchy with $\Delta m = m_5 - m_3 = 100$ GeV for $\sin\alpha = 0.1$ (left) and $\sin\alpha = 0.3$ (right). The excluded regions are shaded with various colors explained in the text. The orange solid line corresponds to the correlation $\sin\alpha = 2\sqrt{3}v_t/v$. The Drell-Yan search channels lose sensitivity beyond the green shaded region where VBF constraints can still provide nontrivial constraints on the parameter space.

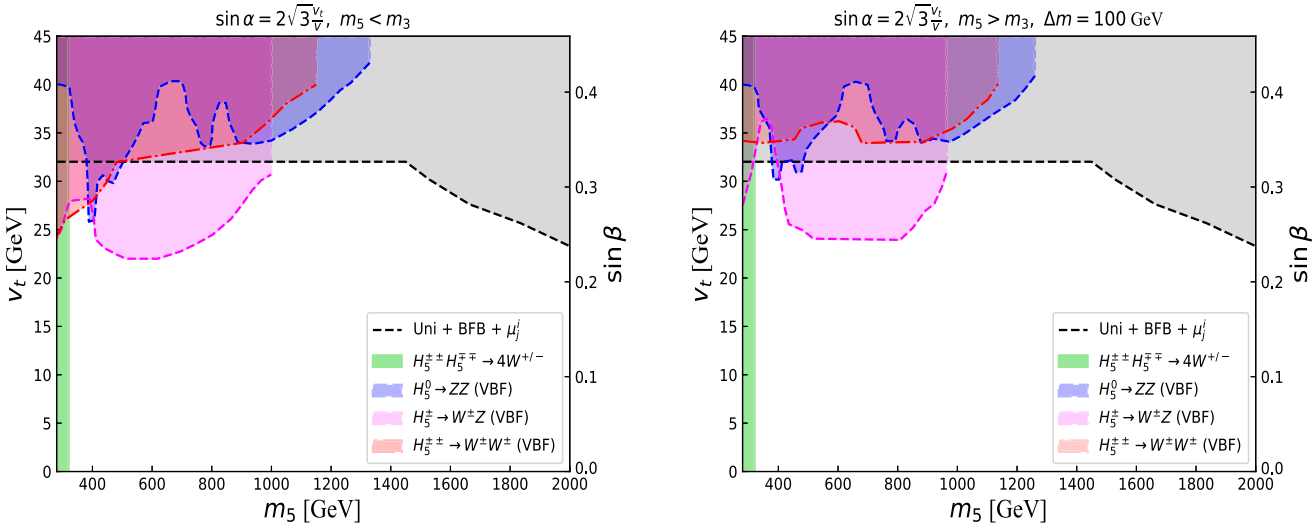

FIG. 6. Combined theoretical and LHC constraints on $m_5 - v_t$ parameter plane for $\sin\alpha$ and v_t correlated as in Eq. (18). The plots correspond to two hierarchies, $m_5 < m_3$ (left) and $m_5 > m_3$ with $(m_5 - m_3) = 100$ GeV (right). The excluded regions are shaded with colors detailed in the text. The Drell-Yan search channels lose sensitivity beyond the green band where VBF constraints can still provide effective constraints on the parameter space.

orange horizontal line, reinforcing the strong correlation between $\sin\alpha$ and v_t as dictated by Eq. (18).[7] We also show the exclusion limit from the searches for Drell-Yan production of $H_5^{\pm\pm}$ decaying to $4W$ final state [19] as a green shaded region. However, the corresponding constraint is much weaker than the others, with masses up to 320 GeV excluded independent of the value of v_t. The limit from the associated Drell-Yan production of $H_5^{\pm\pm}H_5^{\mp}$ [19] is found to be even weaker. Beyond the green band, where the Drell-Yan search becomes ineffective, the VBF searches can still put important constraints on the parameter space. This is a common feature which can be seen in Figs. 5 and 6 as well.

Thus, one can observe from the Fig. 4 that, while the theoretical constraints can most effectively put bounds on the model parameter space towards the high m_5 region, complementary constraints can be provided by the LHC VBF searches for the smaller values of m_5 as well. With the advent of future colliders like the HL-LHC, the collider constraints are expected to cut down deeper into the allowed parameter space towards lower v_t region [63]. Thus, in the absence of any definitive signal of new scalars in the future, triplet contribution to the electroweak VEV will become severely constrained.

[7]In Ref. [20] the bound on the cross section has been reported for nonstandard masses up to 1 TeV. This is why the purple exclusion contours in Figs. 4–6 do not extend beyond 1 TeV.

In addition to direct collider bounds, we also take into account the constraint coming from the measurement of 125 GeV Higgs self-coupling [56]. We evaluate κ_λ according to Eq. (26). The parameter space excluded from the κ_λ constraint is shown as a cyan shaded region. For $\sin\alpha = 0.1$ in the left panel of Fig. 4, the current measurement of κ_λ does not impose any additional constraint on the parameter space. On the other hand, only a marginal additional bound is obtained in the high m_5 region for $\sin\alpha = 0.3$, as can be seen from the cyan shaded region in the right panel of Fig. 4. We would like to mention that κ_λ constraint becomes increasingly more important for larger values of $\sin\alpha(> 0.3)$ and together with the bounds from unitarity and BFB, Higgs signal strength data and direct LHC search limits, it can provide crucial constraints on the large $\sin\alpha$ parameter space.

We do not explicitly show the limits from $H_5^0 \to WW$ in the plots. The bound presented for $H_5^0 \to WW$ via VBF production is much weaker than that of ZZ [21]. Furthermore, we have checked that this particular decay mode has half of the branching fraction to that of $H_5^0 \to ZZ$. Thus, the bounds for $H_5^0 \to WW$ mode provides no additional constraint on our parameter space.

In Fig. 5 we show our allowed parameter region for mass hierarchy $m_5 > m_3$ for two benchmark values of $\sin\alpha$. In this case we present results for $\Delta m = m_5 - m_3 = 100$ GeV, which plays a crucial role in determining the branching ratios of the decaying particles. For $m_5 < m_3$ scenario considered earlier, the only possible decay modes for $H_5^\pm$ are those involving a pair of gauge bosons in the final state. However, here the decay modes of $H_5^\pm$ become more diversified. Additional decays into $H_5^\pm \to H_3^0 W^\pm$, $H_5^\pm \to H_3^\pm Z$ final states are now kinematically accessible, which decreases the signal strengths for $H_5^\pm \to W^\pm Z$ mode, weakening the corresponding bounds. Similarly, the presence of $H_5^0 \to H_3^0 Z, H_3^\pm W^\mp$ modes results in the relaxation of the experimental constraint on H_5^0. Our choice of $\Delta m = 100$ GeV serves as an illustrative benchmark to showcase the relaxation of the collider constraints brought in by the opening up of the additional decay modes.

From Figs. 4 and 5, one may observe a slight variation of the cyan region with m_5, as well as with the hierarchy being considered. This may seem counterintuitive by looking at Eq. (26), which shows no apparent functional dependence of κ_λ on m_5. Such dependence of κ_λ on m_5 is an indirect effect generated by the perturbative unitarity and BFB conditions which correlates the parameters Λ_1 and Λ_2 with values of m_5 and m_3.

In principle, the ATLAS data [18] should also translate as a lower limit on m_H as a function of v_t. Although the $H_5 ZZ$ and HZZ couplings are of similar magnitudes, the width-over-mass ratio for H tends to become large (above 1%) in a significant region of parameter space, not respecting the narrow-width approximation. On the other hand, the $\mathrm{BR}(H \to ZZ)$ gets suppressed in this case because of the presence of various other decays including di-Higgs and fermionic modes that were not present for H_5^0. We have explicitly checked that the effective cross section $\sigma(pp \overset{\mathrm{VBF}}{\to} H \to ZZ)$ lies well below the ATLAS sensitivity reach. The limits on H from $H \to hh$ searches can be effective in constraining parameter spaces with $\sin\beta \gtrsim 0.4$ [29].[8] In our scans, this region lies inside the parameter space already excluded from other complementary constraints.

For the $m_3 < m_5$ hierarchy, the bounds on the charged Higgs boson $H_3^\pm$ must also be taken into account. Out of the two pairs of charged Higgs bosons $H_3^\pm$ and $H_5^\pm$ of the GM model, only the custodial triplet $H_3^\pm$ can couple to the SM fermions through its mixing with the doublet. Thus, $H_3^\pm$ is likely to receive constraints from the charged Higgs boson searches performed at the LHC. The ATLAS collaboration has published search results for the production of charged Higgs bosons decaying to $t\bar{b}$ final state [64]. The corresponding analysis by the CMS collaboration, however, gives a much weaker bound [65]. In GM model the dominant production mode for $H_3^\pm$ is in association with a $t\bar{b}$ pair. There are two possible decay modes for $H_3^\pm$ that dominates its total decay width. $\mathrm{BR}(H_3^\pm \to t\bar{b})$ is dominant for smaller values of m_3. However, $\mathrm{BR}(H_3^\pm \to W^\pm h)$ soon takes over, once it is kinematically allowed [28]. This relaxes the direct search bounds on m_3 from the LHC. In fact, we have explicitly checked that our parameter space of interest lies below the sensitivity region of ATLAS [64] in the $t\bar{b}$ final state.

The pseudoscalar H_3^0 may in principle be subjected to the bounds coming from the LHC searches for a CP-odd neutral scalar decaying into Zh final state [66]. However, these searches target the production of the CP-odd state either in gluon-gluon fusion process or in association with b-quark pairs. Such production modes for H_3^0 suffer a $\mathcal{O}(\sin\beta)$ suppression in our scenario because of the doublet-triplet mixing, making the bound considerably weak. We have checked that the signal yield for this process stays below the limit for all $\sin\alpha$ and $v_t \lesssim 45$ GeV.

In Fig. 6, we explain our results assuming the correlation between $\sin\alpha$ and v_t defined in Eq. (18) to identify the decoupling limit of the model. Compared to Figs. 4 and 5, a significantly larger parameter space is now allowed by the theoretical constraints of unitarity and BFB, especially in the low v_t region. The current measurement of κ_λ does not impose any additional constraints on the parameter space. Once again, one can observe that stronger constraints from the direct collider searches in future will drive v_t to lower

[8]The custodial symmetry forbids couplings of the form $H_5^0 hh$ and $H_3^0 hh$. Also, H_3^0 being a pseudoscalar provides an additional reason not to give rise to the $H_3^0 hh$ coupling.

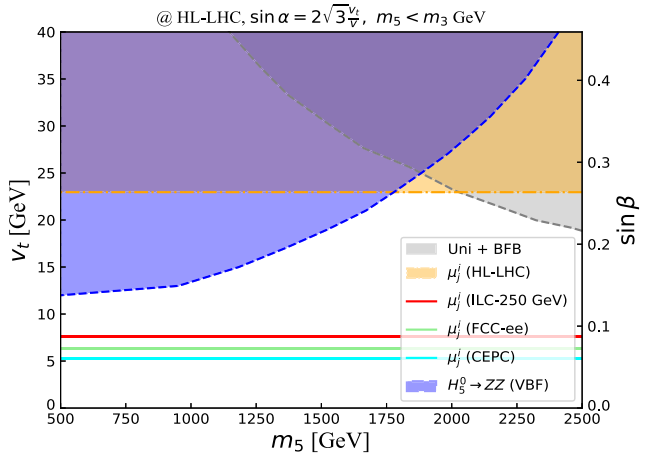

FIG. 7. The expected sensitivity for the HL-LHC assuming the correlation $\sin\alpha = 2\sqrt{3}v_t/v$. The blue shaded area represents the excluded regions from HL-LHC projected limit at $\sqrt{s} = 13$ TeV with integrated luminosity of 3000 fb^{-1} considering the VBF production of H_5^0 and its decay to ZZ [67]. The orange shaded region corresponds to the expected exclusion reach from the HL-LHC measurements of the 125 GeV Higgs signal strength. The corresponding limits from the FCC-ee, CEPC, and International Linear Collider are also shown. The region excluded from the unitarity and BFB constraints is shaded gray. The combined limits from HL-LHC and theoretical constraints will restrict v_t to lower values, driving it closer to the decoupling limit.

values, thereby constantly pushing us towards the decoupling limit.

C. Future prospects: HL-LHC projected limits

Here, we estimate the potential of the upcoming HL-LHC to probe the parameter space of the GM model to a greater extent. In Fig. 7 we present our results assuming the correlation $\sin\alpha = 2\sqrt{3}v_t/v$ for the $m_5 < m_3$ mass hierarchy. The projected sensitivity of HL-LHC searches for the VBF production of a BSM scalar resonance decaying to ZZ mode [67] is used to put constraints on the $m_5 - v_t$ parameter plane. The corresponding exclusion is shown as a blue shaded region. We also show the exclusion from the unitarity and BFB constraints as a gray shaded region. The projected exclusion limit from the HL-LHC measurements of Higgs signal strength is shown as the orange shaded region, assuming the central values of the signal strengths to be consistent with the corresponding SM expectations. Similar limits from the planned Higgs factory experiments [68] like the Future Circular Collider (FCC-ee), the Circular Electron-Positron Collider (CEPC) and the International Linear Collider are also shown in the plot. For the direct searches, one can see almost an order of magnitude improvement in the exclusion bounds compared to the current data, pushing the parameter space down towards lower v_t and hence towards the decoupling limit. On the other hand, even with the projected sensitivity of the HL-LHC to κ_λ, no additional constraints can be obtained on the allowed parameter space for correlated $\sin\alpha$ and v_t. The future Higgs factories can be much more effective in this regard, restricting v_t below 5 GeV. The exclusion contours for the opposite mass hierarchy turn out to be very similar to the one presented here.

V. SUMMARY

In this article, we studied the implications of the nonstandard scalar (neutral as well as charged) searches in the VBF production channel at the LHC, taking the GM model as an illustrative example. The trilinear coupling of a nonstandard scalar with a pair of massive SM gauge bosons should come out to be proportional to the VEV of the electroweak multiplets from which the nonstandard scalar is primarily derived. However, as outlined in the introduction, for models comprising of only $SU(2)_L$ doublets in the scalar sector, the Higgs signal strength measurements force us towards the alignment limit when the SM-like Higgs scalar arises from a particular $SU(2)_L$ doublet in the Higgs basis [5,6], which consumes the entire electroweak VEV. Thus, for these multi-Higgs-doublet models, the trilinear couplings mentioned above become extremely suppressed near the alignment limit. Consequently, the VBF searches for the nonstandard scalars will not be very effective in constraining these multi-Higgs-doublet scenarios.

For models featuring higher $SU(2)_L$ multiplet scalars (in addition to the SM Higgs doublet), the tree level value of the electroweak ρ parameter can get significantly modified. Therefore, the VEV of the additional multiplets may get severely constrained from the precision electroweak measurements. The HTM is a prime example of this scenario when the triplet VEV can, at the most, be of $\mathcal{O}(1\text{ GeV})$. As a result, the trilinear couplings will still be too small to be impactful in the VBF searches for the nonstandard scalars. One may accommodate larger VEVs for the higher $SU(2)_L$ multiplets either by restoring the custodial symmetry [69] or by arranging accidental cancellations [70]. The GM model constitutes an example of the first category where the VEV of the $SU(2)_L$ triplets can be substantially large while still maintaining $\rho = 1$ at the tree level. Thus, it serves as a well-motivated example where the VBF searches can put important constraints on the parameter space especially on the triplet VEV as a function of the common mass of the members of the custodial fiveplet.

In our study of the GM model, we have first analyzed the theoretical constraints from unitarity and BFB. Here we observe that, for low values of the triplet VEV, we need to have a correlation between $\sin\alpha$ and v_t to allow for very heavy nonstandard scalars decoupled from the electroweak scales. The correlation $\sin\alpha \simeq 2\sqrt{3}v_t/v$ grows stronger as the ratio v_t/v becomes smaller. Such a feature seems to have been underemphasized in the literature. Because of this correlation, we systematically approach the SM limit

first by imposing $\sin\alpha = 2\sqrt{3}v_t/v$ and then requiring $v_t \ll v$. We also take into account the constraints coming from the 125 GeV Higgs signal strength measurements.

Next, we study the phenomenological constraints arising from the VBF searches for the nonstandard scalars. Since the members of the custodial fiveplet are derived solely from the component fields of the $SU(2)_L$ triplets [see Eq. (8)], they do not couple to the SM fermions at all and therefore can be exclusively probed via the VBF channels. We have primarily considered the direct searches in the $pp \xrightarrow{\text{VBF}} S \to V_1V_2$ channel. We have explored benchmark scenarios with uncorrelated $\sin\alpha$ and v_t as well as with $\sin\alpha = 2\sqrt{3}v_t/v$. We have found that the LHC constraints can be complementary to the theoretical constraints from unitarity and BFB to constrain the triplet VEV as a function of the custodial fiveplet mass. For $m_5 < m_3$, the upper bound on the triplet VEV can be as strong as $v_t \lesssim 25$ GeV. The relaxation of this bound has also been demonstrated
for the opposite hierarchy, $m_5 > m_3$. With the improved sensitivity projected for the HL-LHC, more stringent constraints on the triplet VEV are expected from the VBF searches, implying that the combination of the direct HL-LHC collider limits and the theoretical constraints will enforce the decoupling limit of the GM model if no deviation from the SM is found in future. Our analysis thus goes to show that the VBF searches for nonstandard scalars can be really useful in restricting the nondoublet contributions to the electroweak VEV and thereby providing valuable intuitions into the constructional aspects of new BSM scenarios. This observation, in turn, underscores the fact that the null results for the BSM searches at the LHC are a lot more than just upper bounds on cross sections as they can be translated into practical insights regarding the anatomy of EWSB.

ACKNOWLEDGMENTS

D. D. thanks the Science and Engineering Research Board, India for financial support through Grant No. CRG/2022/000565. I. S. acknowledges the support from Project No. RF/23-24/1964/PH/NFIG/009073 and from DST-INSPIRE, India, under Grant No. IFA21-PH272. N. G. would like to thank Harish-Chandra Research institute for hospitality and computation facility while the project was going on. N. G. would also like to acknowledge IOE-IISC fellowship program for financial support. S. M. acknowledges Infosys-TIFR leading edge research grant. We also thank the International Centre for Theoretical Sciences (ICTS) for their warm hospitality during the discussion meeting: "Particle Physics: Phenomena, Puzzles, Promises" (code: ICTS/p2p32022/11) where a significant progress of this work has been made.

[1] J. F. Gunion, H. E. Haber, G. L. Kane, and S. Dawson, The higgs hunter's guide, Front. Phys. **80**, 1 (2000).
[2] A. Djouadi, The anatomy of electro-weak symmetry breaking. I: The Higgs boson in the Standard Model, Phys. Rep. **457**, 1 (2008).
[3] J. A. Grifols and A. Mendez, The $WZH^{\pm}$ coupling in $SU(2) \times U(1)$ gauge models, Phys. Rev. D **22**, 1725 (1980).
[4] D. Das and I. Saha, Alignment limit in three Higgs-doublet models, Phys. Rev. D **100**, 035021 (2019).
[5] G. C. Branco, P. M. Ferreira, L. Lavoura, M. N. Rebelo, M. Sher, and J. P. Silva, Theory and phenomenology of two-Higgs-doublet models, Phys. Rep. **516**, 1 (2012).
[6] G. Bhattacharyya and D. Das, Scalar sector of two-Higgs-doublet models: A minireview, Pramana **87**, 40 (2016).
[7] G. Aad *et al.* (ATLAS Collaboration), Observation of a new particle in the search for the Standard Model Higgs boson with the ATLAS detector at the LHC, Phys. Lett. B **716**, 1 (2012).
[8] S. Chatrchyan *et al.* (CMS Collaboration), Observation of a new boson at a mass of 125 GeV with the CMS experiment at the LHC, Phys. Lett. B **716**, 30 (2012).
[9] ATLAS Collaboration, Combined measurements of Higgs boson production and decay using up to 139 fb^{-1} of proton-proton collision data at $\sqrt{s} = 13$ TeV collected with the ATLAS experiment, Report No. ATLAS-CONF-2021-053, 2021.
[10] W. Konetschny and W. Kummer, Nonconservation of total lepton number with scalar bosons, Phys. Lett. **70B**, 433 (1977).
[11] T. P. Cheng and L.-F. Li, Neutrino masses, mixings and oscillations in $SU(2) \times U(1)$ models of electroweak interactions, Phys. Rev. D **22**, 2860 (1980).
[12] S. Kanemura and K. Yagyu, Radiative corrections to electroweak parameters in the Higgs triplet model and implication with the recent Higgs boson searches, Phys. Rev. D **85**, 115009 (2012).
[13] S. Chang, C. A. Newby, N. Raj, and C. Wanotayaroj, Revisiting theories with enhanced Higgs couplings to weak gauge bosons, Phys. Rev. D **86**, 095015 (2012).
[14] H. Georgi and M. Machacek, Doubly charged Higgs bosons, Nucl. Phys. **B262**, 463 (1985).
[15] M. S. Chanowitz and M. Golden, Higgs boson triplets with $M(W) = M(Z)\cos\theta\omega$, Phys. Lett. **165B**, 105 (1985).
[16] J. F. Gunion, R. Vega, and J. Wudka, Higgs triplets in the Standard Model, Phys. Rev. D **42**, 1673 (1990).
[17] G. Aad *et al.* (ATLAS Collaboration), Search for heavy diboson resonances in semileptonic final states in pp collisions at $\sqrt{s} = 13$ TeV with the ATLAS detector, Eur. Phys. J. C **80**, 1165 (2020).

[18] G. Aad *et al.* (ATLAS Collaboration), Search for heavy resonances decaying into a pair of Z bosons in the $\ell^+\ell^-\ell'^+\ell'^-$ and $\ell^+\ell^-\nu\bar{\nu}$ final states using 139 fb^{-1} of proton–proton collisions at $\sqrt{s} = 13$ TeV with the ATLAS detector, Eur. Phys. J. C **81**, 332 (2021).
[19] G. Aad *et al.* (ATLAS Collaboration), Search for doubly and singly charged Higgs bosons decaying into vector bosons in multi-lepton final states with the ATLAS detector using proton-proton collisions at $\sqrt{s} = 13$ TeV, J. High Energy Phys. 06 (2021) 146.
[20] ATLAS Collaboration, Search for resonant $WZ \to \ell\nu\ell'\ell'$ production in proton-proton collisions at $\sqrt{s} = 13$ TeV with the ATLAS detector, Report No. ATLAS-CONF-2022-005, 2022.
[21] ATLAS Collaboration, Search for heavy resonances in the decay channel $\boldsymbol{W + W - e\nu\mu\nu}$ in $\boldsymbol{p\ p}$ Collisions at $\boldsymbol{\sqrt{s}} = 13$ TeV using 139 fb − 1 of data with the ATLAS detector, Report No. ATLAS-CONF-2022-066, 2022.
[22] C.-W. Chiang, A.-L. Kuo, and K. Yagyu, Enhancements of weak gauge boson scattering processes at the CERN LHC, J. High Energy Phys. 10 (2013) 072.
[23] C. Englert, E. Re, and M. Spannowsky, Triplet Higgs boson collider phenomenology after the LHC, Phys. Rev. D **87**, 095014 (2013).
[24] C. Englert, E. Re, and M. Spannowsky, Pinning down Higgs triplets at the LHC, Phys. Rev. D **88**, 035024 (2013).
[25] C.-W. Chiang, S. Kanemura, and K. Yagyu, Novel constraint on the parameter space of the Georgi-Machacek model with current LHC data, Phys. Rev. D **90**, 115025 (2014).
[26] C.-W. Chiang, G. Cottin, and O. Eberhardt, Global fits in the Georgi-Machacek model, Phys. Rev. D **99**, 015001 (2019).
[27] D. Das and I. Saha, Cornering variants of the Georgi-Machacek model using Higgs precision data, Phys. Rev. D **98**, 095010 (2018).
[28] N. Ghosh, S. Ghosh, and I. Saha, Charged Higgs boson searches in the Georgi-Machacek model at the LHC, Phys. Rev. D **101**, 015029 (2020).
[29] A. Ismail, H. E. Logan, and Y. Wu, Updated constraints on the Georgi-Machacek model from LHC Run 2, arXiv: 2003.02272.
[30] A. Ismail, B. Keeshan, H. E. Logan, and Y. Wu, Benchmark for LHC searches for low-mass custodial fiveplet scalars in the Georgi-Machacek model, Phys. Rev. D **103**, 095010 (2021).
[31] T.-K. Chen, C.-W. Chiang, C.-T. Huang, and B.-Q. Lu, Updated constraints on the Georgi-Machacek model and its electroweak phase transition and associated gravitational waves, Phys. Rev. D **106**, 055019 (2022).
[32] C. Wang, J.-Q. Tao, M. A. Shahzad, G.-M. Chen, and S. Gascon-Shotkin, Search for a lighter neutral custodial fiveplet scalar in the Georgi-Machacek model, Chin. Phys. C **46**, 083107 (2022).
[33] S. Ghosh, Fermionic decay of charged Higgs boson in low mass region in Georgi Machacek model, arXiv:2205.03896.
[34] Z. Bairi and A. Ahriche, More constraints on the Georgi-Machacek model, Phys. Rev. D **108**, 055028 (2023).
[35] C. H. de Lima and H. E. Logan, Unavoidable Higgs coupling deviations in the Z_2-symmetric Georgi-Machacek model, Phys. Rev. D **106**, 115020 (2022).
[36] R. Ghosh and B. Mukhopadhyaya, Some new observations for the Georgi-Machacek scenario with triplet Higgs, Phys. Rev. D **107**, 035031 (2023).
[37] A. Ahriche, Constraining the Georgi-Machacek model with a light Higgs boson, Phys. Rev. D **107**, 015006 (2023).
[38] K. Hartling, K. Kumar, and H. E. Logan, The decoupling limit in the Georgi-Machacek model, Phys. Rev. D **90**, 015007 (2014).
[39] C.-W. Chiang and K. Yagyu, Testing the custodial symmetry in the Higgs sector of the Georgi-Machacek model, J. High Energy Phys. 01 (2013) 026.
[40] M. Aoki and S. Kanemura, Unitarity bounds in the Higgs model including triplet fields with custodial symmetry, Phys. Rev. D **77**, 095009 (2008).
[41] D. Das and A. Santamaria, Updated scalar sector constraints in the Higgs triplet model, Phys. Rev. D **94**, 015015 (2016).
[42] J. F. Gunion, H. E. Haber, and J. Wudka, Sum rules for Higgs bosons, Phys. Rev. D **43**, 904 (1991).
[43] B. W. Lee, C. Quigg, and H. B. Thacker, Weak interactions at very high-energies: The role of the Higgs boson mass, Phys. Rev. D **16**, 1519 (1977).
[44] G. Bhattacharyya and D. Das, Nondecoupling of charged scalars in Higgs decay to two photons and symmetries of the scalar potential, Phys. Rev. D **91**, 015005 (2015).
[45] M. Carena, I. Low, N. R. Shah, and C. E. M. Wagner, Impersonating the standard model Higgs boson: Alignment without decoupling, J. High Energy Phys. 04 (2014) 015.
[46] H. E. Logan, Lectures on perturbative unitarity and decoupling in Higgs physics, arXiv:2207.01064.
[47] G. Bhattacharyya, D. Das, P. B. Pal, and M. N. Rebelo, Scalar sector properties of two-Higgs-doublet models with a global U(1) symmetry, J. High Energy Phys. 10 (2013) 081.
[48] M. E. Peskin and T. Takeuchi, Estimation of oblique electroweak corrections, Phys. Rev. D **46**, 381 (1992).
[49] J. F. Gunion, R. Vega, and J. Wudka, Naturalness problems for $\rho = 1$ and other large one loop effects for a Standard Model Higgs sector containing triplet fields, Phys. Rev. D **43**, 2322 (1991).
[50] K. Hartling, K. Kumar, and H. E. Logan, Indirect constraints on the Georgi-Machacek model and implications for Higgs boson couplings, Phys. Rev. D **91**, 015013 (2015).
[51] I. Maksymyk, C. P. Burgess, and D. London, Beyond S, T and U, Phys. Rev. D **50**, 529 (1994).
[52] W. Grimus, L. Lavoura, O. M. Ogreid, and P. Osland, The Oblique parameters in multi-Higgs-doublet models, Nucl. Phys. **B801**, 81 (2008).
[53] R. L. Workman *et al.* (Particle Data Group), Review of particle physics, Prog. Theor. Exp. Phys. **2022**, 083C01 (2022).
[54] CMS Collaboration, A portrait of the Higgs boson by the CMS experiment ten years after the discovery, Nature (London) **607**, 60 (2022).
[55] A. M. Sirunyan *et al.* (CMS Collaboration), Search for charged Higgs bosons produced in vector boson fusion processes and decaying into vector boson pairs in proton–proton collisions at $\sqrt{s} = 13$ TeV, Eur. Phys. J. C **81**, 723 (2021).
[56] ATLAS Collaboration, Constraints on the Higgs boson self-coupling from single- and double-Higgs production with the

ATLAS detector using pp collisions at $s = 13$TeV, Phys. Lett. B **843**, 137745 (2023).
[57] B. Zabinski (ATLAS Collaboration), Probing the nature of electroweak symmetry breaking with Higgs boson pairs in ATLAS, arXiv:2307.11467.
[58] G. Aad *et al.* (ATLAS Collaboration), Search for nonresonant pair production of Higgs bosons in the $bb^{-}bb^{-}$ final state in pp collisions at $s = 13$TeV with the ATLAS detector, Phys. Rev. D **108**, 052003 (2023).
[59] C. Englert, W. Naskar, and D. Sutherland, BSM patterns in scalar-sector coupling modifiers, J. High Energy Phys. 11 (2023) 158.
[60] C. Degrande, C. Duhr, B. Fuks, D. Grellscheid, O. Mattelaer, and T. Reiter, UFO—The Universal FeynRules Output, Comput. Phys. Commun. **183**, 1201 (2012).
[61] N. D. Christensen and C. Duhr, FeynRules—Feynman rules made easy, Comput. Phys. Commun. **180**, 1614 (2009).
[62] A. Alloul, N. D. Christensen, C. Degrande, C. Duhr, and B. Fuks, FeynRules 2.0—A complete toolbox for tree-level phenomenology, Comput. Phys. Commun. **185**, 2250 (2014).
[63] C.-W. Chiang, S. Jana, and D. Sengupta, Investigating new physics models with signature of same-sign diboson $+ + \not{E}_T$, Phys. Rev. D **105**, 055014 (2022).
[64] M. Aaboud *et al.* (ATLAS Collaboration), Search for charged Higgs bosons decaying into top and bottom quarks at $\sqrt{s} = 13$ TeV with the ATLAS detector, J. High Energy Phys. 11 (2018) 085.
[65] CMS Collaboration, Search for charged Higgs bosons decaying into top and a bottom quark in the fully hadronic final state at 13 TeV, Report No. CMS-PAS-HIG-18-015, 2019.
[66] G. Aad *et al.* (ATLAS Collaboration), Search for heavy resonances decaying into a Z or W boson and a Higgs boson in final states with leptons and b-jets in 139 fb^{-1} of pp collisions at $\sqrt{s} = 13$ TeV with the ATLAS detector, J. High Energy Phys. 06 (2023) 016.
[67] M. Cepeda *et al.*, Report from working group 2: Higgs physics at the HL-LHC and HE-LHC, CERN Yellow Rep. Monogr. **7**, 221 (2019).
[68] J. de Blas *et al.*, Higgs boson studies at future particle colliders, J. High Energy Phys. 01 (2020) 139.
[69] A. Kundu, P. Mondal, and P. B. Pal, Custodial symmetry, the Georgi-Machacek model, and other scalar extensions, Phys. Rev. D **105**, 115026 (2022).
[70] C.-W. Chiang and K. Yagyu, Models with higher weak-isospin Higgs multiplets, Phys. Lett. B **786**, 268 (2018).